

# Exploring the electrocatalytic sites of carbon nanotubes for NADH detection: an edge plane pyrolytic graphite electrode study

Craig E. Banks and Richard G. Compton\*

Received 20th June 2005, Accepted 22nd July 2005

First published as an Advance Article on the web 1st August 2005

DOI: 10.1039/b508702c

The electrocatalytic properties of multi-walled carbon nanotube modified electrodes toward the oxidation of NADH are critically evaluated. Carbon nanotube modified electrodes are examined and compared with boron-doped diamond and glassy carbon electrodes, and most importantly, edge plane and basal pyrolytic graphite electrodes. It is found that CNT modified electrodes are no more reactive than edge plane pyrolytic graphite electrodes with the comparison with edge plane and basal plane pyrolytic graphite electrodes allowing the electroactive sites for the electrochemical oxidation of NADH to be unambiguously determined as due to edge plane sites. Using these highly reactive edge plane sites, edge plane pyrolytic graphite electrodes are examined with cyclic voltammetry and amperometry for the electroanalytical determination of NADH. It is demonstrated that a detection limit of 5  $\mu\text{M}$  is possible with cyclic voltammetry or 0.3  $\mu\text{M}$  using amperometry suggesting that edge plane pyrolytic graphite electrodes can conveniently replace carbon nanotube modified glassy carbon electrodes for biosensing applications with the relative advantages of reactivity, cost and simplicity of preparation. We advocate the routine use of edge plane and basal plane pyrolytic graphite electrodes in studies utilising carbon nanotubes particularly if 'electrocatalytic' properties are claimed for the latter.

## Introduction

The electrochemical oxidation of nicotinamide adenine dinucleotide (NADH) is of great interest since it is required in a whole diversity of dehydrogenase-based biosensors; approximately 300 dehydrogenases are known which are dependent on the coenzyme, NADH and its oxidised form  $\text{NAD}^+$ .<sup>1–7</sup> NADH gives an anodic signal at too positive potentials to allow the use of mercury electrodes<sup>8</sup> while the direct oxidation of NADH at unmodified electrode surfaces only proceeds at high (*ca.*  $> +0.5$  V) overpotentials.<sup>3,6</sup> This results in a reduction of the specificity of the electrochemical oxidation of NADH since such a required high overpotential will also oxidise other electroactive species that may be present in the solution being analysed.<sup>3</sup> Another concern is electrode fouling. The oxidised NADH produces  $\text{NAD}^+$  which forms dimers that can adsorb on the electrode surface, hindering heterogeneous charge transfer and resulting in a sensor which becomes inactive as the analysis proceeds, ultimately producing a system which lacks sensitivity.<sup>9–13</sup>

Consequently electrode materials which oxidise NADH at low potentials and which do not lose sensitivity are increasingly sought. A common approach is to modify an electrode surface with a carefully selected mediator; this typically reduces the overpotential and due to the fact that NADH is chemically and indirectly oxidised, the possibility of electrode fouling of the electrode surface is reduced or prevented. Prieto-Simon and Fabregas<sup>3</sup> have systematically studied a range of

commonly used mediators for the oxidation of NADH as well as strategies for incorporating each of the electrocatalysts into a dehydrogenase-based biosensor based on epoxy-graphite composites. They concluded that the optimum immobilisation strategy was to electro-polymerise *o*-phenylenediamine on an epoxy-graphite composite electrode. This was found to produce reproducible surfaces with minimal surface fouling of the electrode with a high sensitivity. However this did not significantly reduce the overpotential which limits the selectivity of the sensor.<sup>3</sup>

A simple and popular methodology in comparison to immobilising mediators at electrode surfaces is to modify an electrode substrate with carbon nanotubes. Wang and coworkers first showed that the electrocatalytic oxidation of NADH at multi- and single-walled CNT modified glassy carbon (GC) electrodes was possible.<sup>13</sup> The authors observed a reduction in the overpotential in comparison to glassy carbon with little electrode fouling. This work was extended by Cai and coworkers who modified GC electrodes with ordered carbon nanotubes achieving a detection limit of 0.5  $\mu\text{M}$ .<sup>14</sup> The authors observed the oxidation of NADH to occur on a bare glassy carbon electrode at +0.645 V *vs.* SCE in phosphate buffer solution (pH 6.8) which decreased to *ca.* 0 V when the ordered CNTs were immobilised onto the GC substrate.<sup>14</sup>

Valentini *et al.* also explored CNT modified GC electrodes which had been modified with poly(1,2-diaminobenzene). An improvement in the electrochemical reversibility of the oxidation of NADH at the polymer-nanotube composition in comparison to a GC electrode modified with poly(1,2-diaminobenzene) was observed which facilitated a detection limit of 50  $\mu\text{M}$ .<sup>15</sup> Valentini *et al.* have also compared the electrochemical reversibility for the oxidation of NADH at

Physical and Theoretical Chemistry Laboratory, Oxford University, South Parks Road, Oxford, UK OX1 3QZ.

E-mail: Richard.Compton@chemistry.ox.ac.uk;

Fax: +44 (0)1865 275410; Tel: +44 (0)1865 275413

carbon paste and carbon nanotube paste electrodes observing the NADH oxidation peak at +466 mV for carbon paste and 546 mV for CN paste electrodes with the CN paste electrode producing a better defined voltammetric wave. Using these electrodes the detection limit was found to be 2  $\mu\text{M}$  in both cases.<sup>16</sup> Liu *et al.* have reported polyaniline carbon nanotube multilayer films supported on gold substrates observing a peak potential around +0.05 V (*vs.* Ag/AgCl) with a detection limit of 1  $\mu\text{M}$ .<sup>17</sup> Carbon nanotubes for NADH sensing have also been utilised in paste electrodes<sup>18,19</sup> and solubilised in biopolymers<sup>20,21</sup> and many additional sensing methodologies for NADH oxidation are likely to be conceived.

Although pyrolytic graphite electrodes have been used to study the electrochemical oxidation of NADH at carbon electrodes by Moiroux and Elving,<sup>8,9,11,12</sup> this was to elucidate the mechanism of oxidation and not for analytical purposes. Furthermore, implicit in the literature is the concept that in respect of basal plane graphite electrodes, electron transfer may be more facile at samples containing a higher proportion of edge plane defects. However we can find no explicit report of studies using an electrode wholly formed of edge plane graphite that is a disc of pyrolytic graphite machined to a chosen diameter with the disc surface facing parallel with the edge plane for the oxidation of NADH. We have recently shown such electrodes to display high electrocatalytic activity for a variety of electroanalytical tasks, including the oxidation of thiols<sup>22</sup> and gas sensing.<sup>23</sup>

In all the above reports using carbon nanotubes, the observed improvement in the oxidation potential of NADH and low susceptibility to electrode fouling has not been explained. In this report we examine the electrochemical oxidation of NADH at carbon nanotube modified electrodes, boron-doped diamond (BDD) and glassy carbon electrodes and compare these responses with those of edge plane and basal plane pyrolytic graphite electrodes allowing the reactive sites of carbon nanotubes to be deduced. Note that this is the first report of using a *bare* edge plane pyrolytic graphite electrode for the electroanalytical detection of NADH oxidation. This facilitates a detection limit of 5  $\mu\text{M}$  *via* cyclic voltammetry or 0.3  $\mu\text{M}$  with amperometry.

## Experimental

All chemicals used were of analytical grade and used as received without any further purification.  $\beta$ -Nicotinamide adenine dinucleotide, reduced disodium salt hydrate, (NADH > 98%) was obtained from Sigma.

Solutions were prepared with deionised water of resistivity not less than 18.2 M $\Omega$  cm (Millipore water systems, UK). Voltammetric measurements were carried out using a  $\mu$ -Autolab II potentiostat (Eco-Chemie, The Netherlands) with a three-electrode configuration.

Multi-walled carbon nanotubes (purity >95%, diameter  $30 \pm 15$  nm, length 5–20  $\mu\text{m}$ ) were purchased from Nano-Lab Inc. (Bright, MA, USA) and used without any further purification. These are purchased in two forms, “Bamboo” and “Hollow-tube”. In the latter the axis of the graphite planes are parallel to the axis of the nanotube, while in the former, the graphite planes are formed at an angle to the axis of the tube

where the nanotubes are periodically closed along the length of the tube into compartments rather like bamboo or a stack of paper cups fitted one inside the other.

Edge and basal plane pyrolytic graphite, (eppg, bppg, Le Carbone, Ltd. Sussex, UK) BDD and GC (3 mm diameter, BAS Technicol, USA) were used as working electrodes. In the former case discs of pyrolytic graphite were machined into a 4.9 mm diameter, which was oriented with the disc face parallel with the edge plane, or basal plane as required. The counter electrode was a bright platinum wire, with a saturated calomel electrode completing the circuit. The working electrodes were polished on alumina lapping compounds (BDH) of decreasing sizes (0.1–5  $\mu\text{m}$ ) on soft lapping pads.

The basal plane pyrolytic graphite electrodes were modified with MWCNT by ‘film’ and abrasive modification; the former is produced by taking a prepared bppg electrode and pipetting a micro-litre suspension of the desired CNTs onto the electrode surface and allowing the slurry to evaporate at room temperature. In the latter case, the prepared bppg is gently rubbed on a piece of filter paper along with the desired CNTs.

All experiments were typically conducted at  $20 \pm 2$  °C. Before commencing experiments, nitrogen (BOC, Guildford, Surrey, UK) was used for deaeration of solutions.

A 0.1 M phosphate buffer (0.05 M  $\text{NaH}_2\text{PO}_4$  + 0.05 M  $\text{Na}_2\text{HPO}_4$  adjusted to pH 7.4) solution was used throughout this work since enzyme-catalysed reactions of NADH and NADPH-dependent dehydrogenases are pH dependent with pH optimal at pH 7 and above; consequently it is important to develop working electrodes for use at pH 7 and this is reflected in the choice of pH used in experiments reported in the literature.<sup>6</sup>

## Results and discussion

### Comparison of electrode substrates for the electrochemical oxidation of NADH

Fig. 1 depicts the cyclic voltammetric responses from the electrochemical oxidation of 1.2 mM NADH at edge plane pyrolytic graphite (A), boron-doped diamond (B) and glassy carbon (C) electrodes in a pH 7.4 phosphate buffer solution, recorded over a range of scan rates. A similar voltammetric response is observed on both the glassy carbon and boron-doped diamond electrodes with the electrochemical oxidation of NADH occurring with peak potentials of *ca.* +0.55 and *ca.* +0.53 V respectively (*vs.* SCE, 50  $\text{mV s}^{-1}$ ). These potentials are in agreement with literature reports but it is worth noting that GC electrodes have been reported widely in the literature to be highly susceptible to electrode passivation from the strong adsorption of the  $\text{NAD}^+$  produced at the electrode from the oxidation of NADH.<sup>1,2,13</sup> For example Pariente *et al.* observed a 300 mV positive shift<sup>2</sup> due to adsorption processes at GC electrodes. It is interesting to note that BDD has been reported as having a high resistance to such electrode fouling.<sup>1</sup> It is thought that the lack of polar oxygen-containing functional groups on the surface of the BDD electrode is responsible for the lack of adsorption and resistance to fouling by  $\text{NAD}^+$ .<sup>1,24</sup>

In comparison to both the BDD and GC electrodes, the eppg electrode exhibits a shift in potential to a less positive

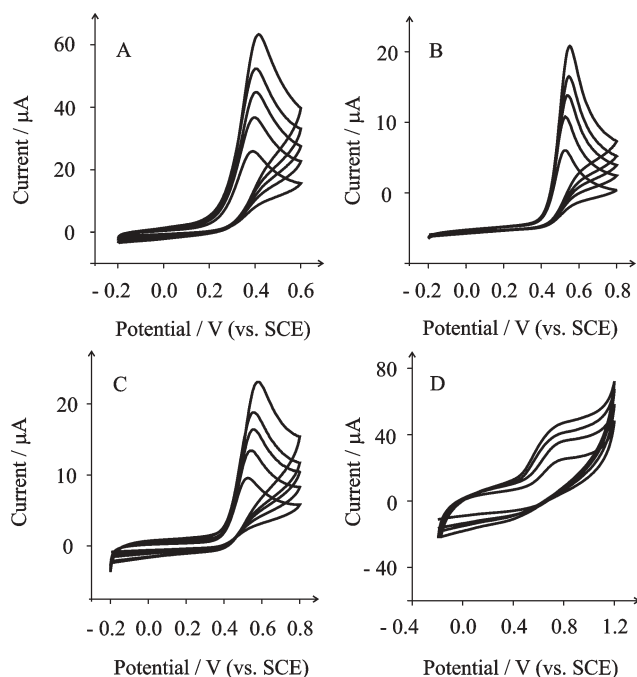


**Fig. 1** The cyclic voltammetric responses of (A) edge plane pyrolytic graphite, (B) boron-doped diamond, (C) glassy carbon and (D) basal plane pyrolytic graphite electrodes in a pH 7.4 phosphate buffer solution containing 1.2 mM NADH. The scan rates used were 25, 50, 75, 100 and 150  $\text{mV s}^{-1}$ .

value which is evident from the defined peak at *ca.* +0.40 V (*vs.* SCE, 50  $\text{mV s}^{-1}$ ) as shown in Fig. 1A. Next the voltammetric response of a basal plane pyrolytic graphite electrode was examined for electrochemical oxidation of NADH. Using the same solution composition as above, an oxidation wave, which is shown in Fig. 1 D, is observed to occur at *ca.* +0.81 V (*vs.* SCE, 50  $\text{mV s}^{-1}$ ). As discussed in the introduction, edge plane graphite exhibits faster heterogeneous electron transfer than basal plane graphite, such that in the case of a heterogeneous electrode the edge plane sites are the predominant sites for electron transfer to occur.<sup>25</sup> This bppg electrode has been prepared such that little edge plane graphite is present; this allows us to infer where the electrochemical reactivity originates. The high proportion of basal plane, *i.e.* low edge plane density, produces a voltammetric profile as observed in Fig. 1D which occurs at a high overpotential due to the slow electrode kinetics and limited amount of edge plane sites on the electrode surface.

In Fig. 1 the observed voltammetric response is due to the electrochemical oxidation of NADH:<sup>9,12,26</sup>



Tafel analysis of voltammograms recorded at the eppg electrode corresponding to the oxidation of 1.2 mM NADH (at a scan rate of 100  $\text{mV s}^{-1}$ ) plotted as potential *vs.*  $\log_{10}(\text{current})$  produced a value of 167 mV per decade. Using the following equation:

$$y = \frac{2.303RT}{\alpha n_a F} \quad (2)$$

where  $y$  (V) is the slope of potential *vs.*  $\log_{10}(\text{current})$ ,  $\alpha$  is the transfer coefficient for the potential-determining heterogeneous electron transfer and  $n_a$  is the number of electrons transferred in the rate determining step. A value of 0.35 for  $\alpha n_a$  was obtained suggesting that in the overall two electron oxidation of NADH, the first electron transfer is the rate determining step. This transfer coefficient is consistent with that observed by Moiroux and Elving,<sup>12</sup> who observed transfer coefficients of 0.37 at carbon electrodes and 0.43 at platinum electrodes for the electrochemical oxidation of NADH. The lower than expected value (usually 0.5) is perhaps not unexpected since the value results from a dissymmetry of the potential energy curves of the reactant and products in the context of Butler–Volmer kinetics suggesting that the irreversibility of the first electron transfer (rate determining step) is the likely cause of the observed large overpotential for the electrochemical oxidation of NADH.

As shown in Fig. 1 the scan rate dependence of the voltammetric response at all the electrode substrates was explored. As can be observed in Fig. 1, the oxidation peak potential shifts with increasing scan rates towards a more positive potential, confirming the electrochemical irreversibility of the electrochemical reaction. For the eppg electrode a plot of peak height ( $I_H$ ) against square root of scan rate (10–150  $\text{mV s}^{-1}$ ) was constructed, which was found to be linear ( $I_H/A = 1.56 \times 10^{-4} \text{V}^{-1/2} \text{s}^{-1/2}$ ), suggesting that the process is diffusion rather than surface controlled. From this plot an approximate diffusion coefficient can be calculated using the following equation for a diffusion controlled electrochemically irreversible reaction in which the first electron transfer is rate-determining:

$$I_{\text{peak}} = (2.99 \times 10^5) A C_0 D^{1/2} v^{1/2} n(\alpha n_a)^{1/2} \quad (3)$$

where  $n$  is the total number of electrons in the overall oxidation of NADH which is 2,  $D$  is the diffusion coefficient,  $C_0$  is the bulk concentration,  $A$  is the electrode area,  $v$  is the scan rate, with values for  $\alpha$  and  $n_a$  which are deduced from eqn (2) were 0.35 and 1 respectively. This produced an approximate value for the diffusion coefficient to be  $3.8 \times 10^{-6} \text{cm}^2 \text{s}^{-1}$ . This value compares with reported values of  $6.7 \times 10^{-6} \text{cm}^2 \text{s}^{-1}$  in 0.005 M phosphate buffer (pH 7),<sup>27</sup>  $3.24 \times 10^{-6} \text{cm}^2 \text{s}^{-1}$  in 0.1 M phosphate buffer (pH 7),<sup>28</sup>  $2.4 \times 10^{-6} \text{cm}^2 \text{s}^{-1}$  in 0.05 M phosphate buffer (pH 7) containing 0.1 M  $\text{KCl}^5$  and  $2.3 \times 10^{-6} \text{cm}^2 \text{s}^{-1}$  in 0.5 M  $\text{KCl}$  plus 0.05 M Tris buffer (pH 7.1). The wide diversity probably reflects the occurrence of adsorption effects as described above.

The mechanism of the oxidation of NADH is thought to be the following:<sup>12</sup>



where NADH is irreversibly oxidised through loss of an electron to produce a cation radical  $\text{NADH}^{\bullet+}$  eqn (4), which then de-protonates to produce a neutral radical  $\text{NAD}^{\bullet}$  eqn (5).  $\text{NAD}^{\bullet}$  is immediately oxidised to  $\text{NAD}^+$  at the electrode

surface at the positive potential involved (typically 0.5 V) as described by eqn (6).  $\text{NAD}^+$  can also exchange an electron with the cation radical in the bulk solution.<sup>12</sup>

### Comparison of MW-CNT modified electrodes with edge plane and basal plane pyrolytic graphite electrodes for the electrochemical oxidation of NADH

Recently we demonstrated that the electrochemical reactivity of multi-walled carbon nanotubes (MWCNT) is due to edge plane defects which occur at the open-ends of the nanotube and around the tube walls where one of the concentric tubes terminates.<sup>29</sup> Numerous reports of the low-potential detection of NADH at carbon nanotube modified electrodes have been reported as discussed in the introduction; it is therefore pertinent to compare the oxidation of NADH at carbon nanotube modified electrodes with that at edge plane and basal plane pyrolytic graphite electrodes.

In this study basal plane pyrolytic graphite electrodes were modified with MWCNT by 'film' and abrasive modification (see experimental section for details). Fig. 2A and B depict the responses of the abrasive and film modified carbon nanotube bppg electrodes respectively. Two distinct voltammetric profiles are observed as a result of modification; we consider each in turn.

We first consider the response of the (hollow-tube) MWCNTs abrasively modified bppg electrode, where two

oxidation waves are observed at *ca.* +0.31 V and *ca.* +0.48 V (both *vs.* SCE, 50  $\text{mV s}^{-1}$ ) as shown in Fig. 2A. This response is similar to that reported by Wang and coworkers<sup>13</sup> who explored the oxidation of NADH at a film modified MWCNT GC electrode. The authors observed an oxidation peak at +0.33 V in pH 7.4 buffer recorded at 50  $\text{mV s}^{-1}$  with a second less defined oxidation process at +0.57 V, both *vs.* Ag/AgCl. The potential of the Ag/AgCl reference electrode is  $-0.045$  V relative to the saturated calomel electrode<sup>30</sup> and if we correct our observed peak potentials (+0.31 V and +0.48 V, *vs.* SCE, 50  $\text{mV s}^{-1}$ ) to coincide with the reference electrode used by Wang and coworkers<sup>13</sup> we find that the oxidation of NADH in this study occurs at +0.27 V with the apparent second oxidation wave at +0.43 V. The main oxidation wave observed at the CNT abrasively modified bppg (+0.27 V, shown in Fig. 2A) is in excellent agreement, albeit at a slightly less positive potential, with that observed by Wang and coworkers<sup>13</sup> (+0.33 V).

Next we consider the response of the MWCNT film modified bppg electrode (Fig. 2B) for the electrochemical oxidation of NADH. The response is typical of carbon nanotube electrode modified *via* the method where 'thin layer' behaviour is observed with the loss of the 'diffusional tail'.<sup>31</sup> In comparison to the abrasively modified electrode discussed above, a single oxidation wave is observed at +0.30 V (*vs.* SCE, 50  $\text{mV s}^{-1}$ ). This corresponds to +0.26 V if we correct this relative to the Ag/AgCl reference electrode which again, is slightly less positive than that reported previously.<sup>13</sup> Note that the MWCNTs used above are termed 'hollow-tube'. A bppg electrode was prepared as described above and modified with 'bamboo' MWCNTs *via* film and abrasive attachment. A identical response was observed with the film modified nanotubes exhibiting an oxidation wave at *ca.* +0.3 V while two waves were observed at *ca.* +0.32 and *ca.* +0.55 V at the abrasively modified bppg electrode (all *vs.* SCE, 50  $\text{mV s}^{-1}$ ). It is interesting to note that the second wave is not observed on the MWCNT film modified bppg electrodes suggesting that this is due to the response of the underlying electrode. The origin of the apparent second oxidation wave observed at the abrasively modified MWCNTs bppg electrodes is discussed below.

In the present study the bppg electrode which consists of very little edge plane is shown in Fig. 2C curve i, where the oxidation wave is observed at *ca.* +0.81 V. The bppg was then polished on a soft lapping pad with 0.1 micron sized alumina for 10 and 30 seconds. The polished bppg electrode was then placed into the NADH solution with the voltammetric response found to occur at *ca.* +0.41 (Fig. 2C curve ii) and *ca.* +0.46 V (Fig. 2C curve iii). The effect of increasing scan rate on the voltammetric response after polishing the bppg electrode on alumina for 30 seconds is shown in Fig. 2D, which is similar to the eppg response (see Fig. 1A). Abrasive rubbing of the bppg on the alumina introduces edge plane defects on the electrode surface which result in a shift of the oxidation wave to less negative potentials with a reduction in the background current, because the kinetics on the edge plane sites are considerably faster.<sup>32</sup> In fact it has been shown through numerical simulations and comparison with experiments, that the basal plane is effectively *electrochemically inert*; a bppg electrode which has been adhesively prepared (see

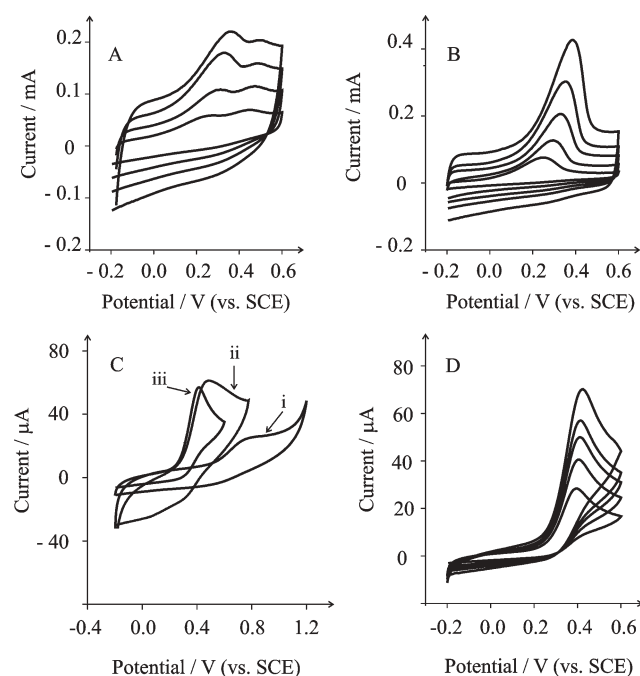


**Fig. 2** The cyclic voltammetric response of (A) abrasively modified MWCNT bppg and (B) film modified MWCNTs on bppg electrodes in a pH 7.4 phosphate buffer solution containing 1.2 mM NADH. All scans are 25, 50, 75, 100 and 150  $\text{mV s}^{-1}$ . Shown in (C) is the response of a bppg electrode (curve i) and after polishing the electrode on a soft lapping pad with 0.1 micron-sized alumina for 10 (curve ii) and 30 seconds (curve iii). The response of increasing scan rate is shown in (D) after polishing a bppg electrode with 0.1 micron alumina for 30 seconds.

experimental section) has a percentage of edge plane defects between 1–10% which is increased by abrasive modification.<sup>25</sup>

We therefore infer that the second wave observed only on the abrasive CNT modified bppg electrode Fig. 2A is due to the nanotubes abrasively roughening the bppg electrode which introduces edge plane sites. Thus two waves are produced, the first from the high proportion of edge plane sites occurring on the carbon nanotubes and the second from electron transfer from the relatively smaller proportion of edge plane sites from the bppg electrode surface.<sup>29,32</sup>

Thus it is highly likely that the two wave response observed by Wang and coworkers<sup>13</sup> for NADH oxidation at MWCNT 'film' modified glassy carbon electrodes is due to the edge plane sites on the CNTs and those of the underlying glassy carbon electrode.

In a comparison of the response of the eppg electrode with that of the MWCNTs, the oxidation of NADH at carbon nanotubes occurs at a slightly less positive potential (*ca.* +0.30 V) than that of the edge plane pyrolytic response (*ca.* +0.40 V). This is likely due to the higher number per square centimetre of edge plane sites on the carbon nanotubes in comparison to the eppg electrode. This is in agreement with Lawrence *et al.*<sup>33</sup> who explored a range of commercially available carbon nanotubes obtained from different sources where it was found that Nanolab chemical vapour deposition produced CNTs that were more electrochemically reactive than those made using an ARC discharge methodology. This was guessed by the authors to be due to the higher density of edge plane defects occurring on the CVD fabricated CNTs in comparison to the ARC produced CNTs.<sup>33</sup> Our study unambiguously confirms the authors suspicions on the role of edge plane sites in their work.

We next turn to exploring the stability of the electrodes in respect of surface fouling from  $\text{NAD}^+$  which is formed from the oxidation of NADH (see eqn 4). The voltammetric response of each of the electrode substrates before, and after, being left in a 1.1 mM solution of NADH for 30 minutes was explored. The results are depicted in Fig. 3. The response at the boron-doped diamond (Fig. 3A) after being left in the solution for 30 min resulted in the oxidation wave of NADH shifting by *ca.* 80 mV to a more positive potential with a decrease in the peak height and slight increase in background current, while for the edge plane pyrolytic graphite (Fig. 3B) only a relatively small decrease in peak height is observed. For the abrasively modified MWCNT bppg electrode (Fig. 3C) a decrease in peak height and a slight potential shift by *ca.* 20 mV positive is observed in comparison to the response at the film modified MWCNT bppg electrode (Fig. 3D) where only the peak height is observed to decrease. In the above, the decrease in peak height and potential shift to more positive values is indicative of adsorption phenomena, which has been widely reported to happen at glassy carbon substrates.<sup>1,13</sup>

Of all the above electrode substrates tested, it would appear that only the film modified MWCNT bppg electrode and the edge plane pyrolytic graphite electrode could be successfully utilised in dehydrogenase sensors. The response at the bppg electrode sheds some light on this. Fig. 3E shows the response of the bppg electrode before (dashed line) and after (solid line) being left in the NADH solution for 30 minutes. In the former

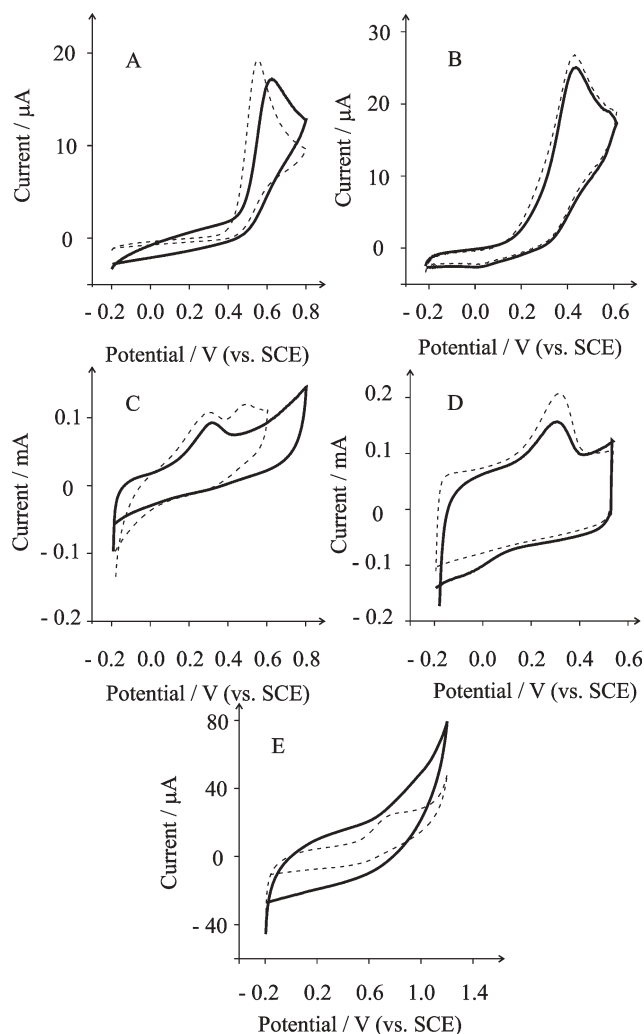


**Fig. 3** Voltammetric responses before (dashed line) and after (solid line) leaving boron-doped diamond (A), edge plane pyrolytic (B), abrasively modified MWCNT bppg (C), film modified MWCNT bppg (D) and bppg (E) electrodes in a pH 7.4 phosphate buffer solution containing 1.1 mM NADH for 30 minutes. Note that the response of the oxidation of NADH at the electrode substrates were first sought. The electrodes were then left in the same solution for 30 min, after which the solution was stirred with the oxidation of NADH again explored.

case, as discussed above, the electrochemical response is due to the very small proportion of edge plane sites and results in a voltammetric wave at a high overpotential in comparison to an electrode consisting solely of edge plane. In the latter case, after the 30 minute period, no visible voltammetric waves are observed in the accessible potential window. It can be inferred that  $\text{NAD}^+$  has adsorbed at the edge plane sites (after the 30 min period) such that the electrode response (which is the oxidation of NADH to  $\text{NAD}^+$ ) is completely dominated by basal plane sites. As mentioned above, these sites exhibit very slow electron transfer kinetics, thus resulting in either no voltammetric response, or a response at such a high overpotential that it is outside the electrochemical window. The observation that  $\text{NAD}^+$  adsorbs on edge plane sites is similar to the reported behaviour of boron-doped diamond and glassy

carbon substrates. In the case of the edge plane pyrolytic graphite electrode and the film modified MWCNT bppg electrode the adsorption of  $\text{NAD}^+$  at these edge plane sites (open ends or tube defects for CNTs) is observed by the decrease in peak height. If adsorption occurred solely at basal plane sites, the response of the bppg electrode in Fig. 3E would be the inverse of what is seen, possibly with little or no charge being passed, while for the eppg electrode and the MWCNT film modified bppg electrode no difference would be seen after leaving the electrodes in the NADH solution for 30 minutes. All the above evidence points to the edge plane sites as the location(s) where adsorption takes place. However this has not been shown hitherto in the literature but explains the superiority of carbon nanotubes and edge plane pyrolytic graphite electrodes over other carbon based electrodes commonly used in sensing applications.

### Cyclic voltammetric and amperometric detection of NADH at edge plane pyrolytic graphite electrodes

We next turn to exploring the sensing possibilities of the edge plane pyrolytic graphite electrode using cyclic voltammetry and amperometry.

Using a pH 7.4 phosphate buffer solution, additions of  $4.1 \mu\text{M}$  NADH were made with the voltammetric response explored using a scan rate of  $100 \text{ mV s}^{-1}$ . The cyclic voltammograms are shown in Fig. 4 along with a resulting calibration plot. Note also that the response of  $8.1 \mu\text{M}$  NADH is also

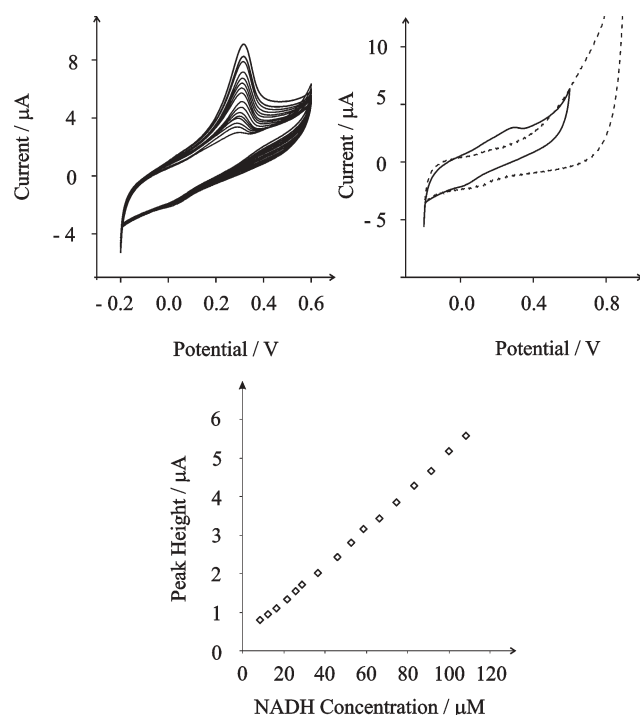


**Fig. 4** Voltammetric response observed at the edge plane pyrolytic graphite electrode from additions of  $4.1 \mu\text{M}$  NADH to a pH 7.4 phosphate buffer solution from  $8.2 \mu\text{M}$  to  $108 \mu\text{M}$  (top left) with a typical calibration plot of peak height versus added NADH concentration from the voltammetric responses. Also shown (top right) is the voltammetric response from the addition of  $8.1 \mu\text{M}$  to the solution along with the corresponding blank (dashed line).

shown, where a large and quantifiable signal is observed which can be easily distinguished from the blank. Analysis of the voltammetric curves from additions of NADH showed a linear response from  $8.3 \mu\text{M}$  to  $108 \mu\text{M}$  with a plot of peak height ( $I_H$ ) versus added NADH producing the following linear regression:  $I_H/A = 4.9 \times 10^{-2}([\text{NADH}]/\text{M}) + 3.6 \times 10^{-7}A$ ;  $R^2 = 0.98$ ,  $N = 16$ ). The peak height is measured by placing a baseline just before the start of the oxidation wave (ca.  $0.1 \text{ V}$ ) to just after the end of the oxidation wave. The peak height is then the difference between the baseline and the peak maximum. From the calibration plot, a limit of detection, based on a signal-to-noise ratio of  $3\sigma$  was found to be  $4.5 \mu\text{M}$ .

Next the amperometric response of the edge plane pyrolytic graphite electrode was explored. Fig. 5 depicts the current-time response from additions of NADH to a pH 7.4 phosphate buffer solution under conditions where the potential was kept at  $+0.4 \text{ V}$ . As shown successive additions from  $2.25 \mu\text{M}$  to  $36 \mu\text{M}$  produced a well-defined response producing the following linear regression:  $I/A = 5.46 \times 10^{-2}([\text{NADH}]/\text{M}) + 8.34 \times 10^{-8}A$ ;  $N = 16$ ;  $R^2 = 0.997$ ; the plot of current versus NADH concentration is shown in Fig. 5. From this graph a limit of detection ( $3\sigma$ ) of  $9.65 \times 10^{-7} \text{ M}$  was calculated. Note that with each addition of NADH a response time of less than 1 second is observed with a sharp rise in the current. This experiment was repeated, but with smaller additions over the range  $0.9$  to  $10.8 \mu\text{M}$  ( $I/A = 6.4 \times 10^{-2}([\text{NADH}]/\text{M}) - 3.1 \times 10^{-8}A$ ;  $N = 12$ ;  $R^2 = 0.997$ ) and was found to

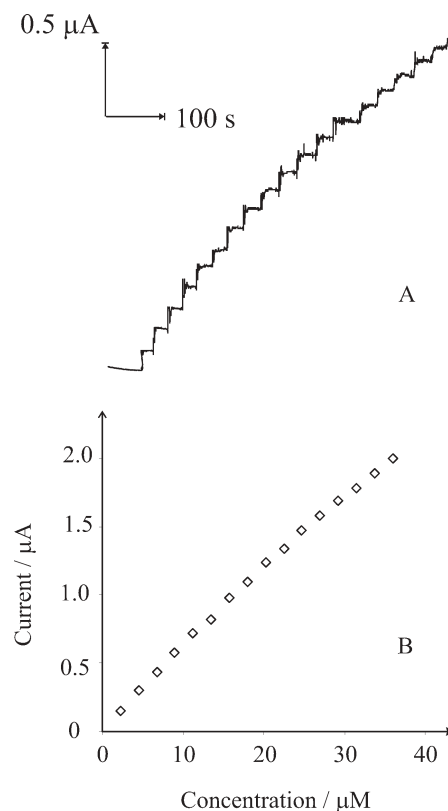


**Fig. 5** Amperometric response observed at the edge plane pyrolytic graphite electrode from  $2.25 \mu\text{M}$  NADH additions to a pH 7.4 phosphate buffer solution at a rotating ( $13 \text{ Hz}$ ) edge plane pyrolytic graphite electrode. Operating potential,  $+0.4 \text{ V}$  (vs. SCE).

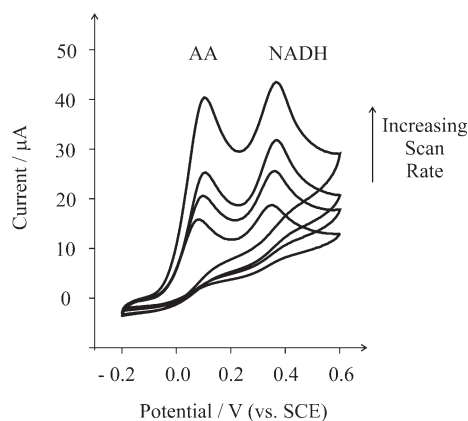


**Fig. 6** Voltammetric responses of an edge plane pyrolytic graphite electrode in a pH 7.4 phosphate buffer solution containing 500  $\mu\text{M}$  ascorbic acid and NADH. Scans conducted at 25, 50, 75 and 100  $\text{mV s}^{-1}$ .

produce a limit of detection of  $3.3 \times 10^{-7}$  M. The detection limits from cyclic voltammetry and amperometry are comparable to existing methods employing carbon nanotubes<sup>13,14,18</sup> and nanotube polymer composites.<sup>15,17,21</sup> Note that the detection limits achievable above are better than GC electrodes modified with transition metal complexes,<sup>7,34</sup> electroactive dyes,<sup>35–37</sup> quinone functional mediators<sup>38</sup> and poly(thionine) modified carbon electrodes.<sup>39</sup>

The edge plane pyrolytic graphite electrode has the advantage of simplicity for routine sensing of NADH over carbon nanotube modified electrodes and may be used as an alternative to the latter. For optimum dehydrogenase sensors, it is recommended that the carbon surface of the working electrode has a high density of edge plane sites by using either an eppg electrode, a polished bppg or a carbon nanotube modified electrode/composite.

Ascorbic acid (AA) is one of the largest problems in the electrochemical determination of biological substances such as NADH since AA is commonly oxidised at similar potentials. One way to alleviate this is to apply a membrane such as Nafion which electrostatically excludes anions such as ascorbate.<sup>1</sup> However this is not without its drawbacks since a reduction in the sensitivity is all too often observed.<sup>1</sup> We have consequently examined the oxidation of NADH in the presence of AA at the edge plane pyrolytic graphite electrode. Fig. 6 shows the cyclic voltammetric responses of equal concentrations of AA and NADH in a pH 7.4 phosphate buffer solution. The peak at +0.11 V (*vs.* SCE) is due to the electro-oxidation of ascorbic acid with the NADH signal at +0.37 V (*vs.* SCE); this equates to a peak separation of 260 mV. Note that the peak separation of AA and NADH has been observed to be *ca.* 130 mV (pH 7.1) at boron-doped diamond electrodes, which was too small to give resolved voltammetric peaks with the presence of AA being observed as a shoulder on the NADH peak.<sup>1</sup> Note that this must be due to the oxidation of AA exhibiting a higher degree of electrochemical reversibility at the eppg in comparison to BDD electrodes. Fig. 6 suggests that eppg electrodes can be used without any interference from ascorbic acid when used in conjunction with cyclic voltammetry.

## Conclusions

The response of an edge plane pyrolytic graphite electrode for the sensing of NADH has been explored and compared with basal plane pyrolytic graphite, glassy carbon, boron-doped diamond and MWCNT modified bppg electrodes. This has allowed the following insights.

1) The electrocatalytic properties of multi-walled carbon nanotube modified electrodes toward the oxidation of NADH are shown to be due edge plane sites/defects which occur along the tube axis or at the open ends of the tubes, with ‘hollow-tube’ and ‘bamboo’ type nanotubes giving similar responses.

2) The adsorption of NADH at CNTs and edge plane electrodes occurs at edge plane sites. Due to the high density of edge plane sites on CNTs and edge plane pyrolytic graphite electrodes, they are unsusceptible to electrode passivation. The oxygen functionalities may likely reside here and promote a means for binding the adsorbing materials.

3) Electroanalytical sensors utilizing carbon based electrodes should optimally have a large proportion of edge plane sites for the best detection limits and,

4) edge plane pyrolytic graphite electrodes can conveniently replace carbon nanotube modified electrodes for routine sensing of NADH due to their simplicity of preparation, low susceptibility to electrode fouling, low detection limit and insensitivity to interference from AA.

## References

- 1 T. N. Rao, I. Yagi, T. Miwa, D. A. Tryk and A. Fujishima, *Anal. Chem.*, 1999, **71**, 2506.
- 2 F. Pariente, F. Tobalina, G. Moreno, L. Hernandez, E. Lorenzo and H. D. Abruna, *Anal. Chem.*, 1997, **69**, 4065.
- 3 B. Prieto-Simon and E. Fabregas, *Biosens. Bioelectron.*, 2004, **19**, 1131.
- 4 C. O. Schmamel, K. S. V. Santhanam and P. J. Elving, *J. Am. Chem. Soc.*, 1975, **97**, 5083.
- 5 J.-J. Sun, J.-J. Xu, H.-Q. Fang and H.-Y. Chen, *Bioelectrochem. Bioenerg.*, 1997, **44**, 45.
- 6 P. N. Barlett, P. R. Birkin and E. N. K. Wallace, *J. Chem. Soc., Faraday Trans.*, 1997, **93**, 1951.
- 7 Q. Wu, M. Maskus, F. Pariente, F. Tobalina, V. M. Fernandez, E. Lorenzo and H. D. Abruna, *Anal. Chem.*, 1996, **68**, 3688.
- 8 J. Moiroux and P. J. Elving, *Anal. Chem.*, 1978, **50**, 1056.
- 9 J. Moiroux and P. J. Elving, *J. Electroanal. Chem.*, 1979, **102**, 93.
- 10 M. A. Hayes and W. G. Kuhr, *Anal. Chem.*, 1999, **71**, 1720.
- 11 J. Moiroux and P. J. Elving, *Anal. Chem.*, 1979, **51**, 346.
- 12 J. Moiroux and P. J. Elving, *J. Am. Chem. Soc.*, 1980, **102**, 6533.
- 13 M. Musameh, J. Wang, A. Merkoci and Y. Lin, *Electrochem. Commun.*, 2002, **4**, 743.
- 14 J. Chen, J. Bao, C. Cai and T. Lu, *Anal. Chim. Acta*, 2004, **516**, 29.
- 15 F. Valentini, A. Salis, A. Curulli and G. Palleschi, *Anal. Chem.*, 2004, **76**, 3244.
- 16 F. Valentini, S. Orlanducci, M. L. Terranova, A. Amine and G. Palleschi, *Sens. Actuators, B*, 2004, **100**, 117.
- 17 J. Liu, S. Tian and W. Knoll, *Langmuir*, 2005, **21**, 5596.
- 18 R. Antiochia, I. Lavagnini and F. Mago, *Anal. Bioanal. Chem.*, 2005, **381**, 1355.
- 19 M. D. Rubianes and G. A. Rivas, *Electroanalysis*, 2005, **17**, 73.
- 20 M. Zhang and W. Gorski, *J. Am. Chem. Soc.*, 2005, **127**, 2058.
- 21 M. Zhang, A. Smith and W. Gorski, *Anal. Chem.*, 2004, **76**, 5045.
- 22 R. R. Moore, C. E. Banks and R. G. Compton, *Analyst*, 2004, **129**, 755.
- 23 C. E. Banks, A. Goodwin, C. G. R. Heald and R. G. Compton, *Analyst*, 2005, **130**, 280.
- 24 J. Xu, Q. Chen and G. M. Swain, *Anal. Chem.*, 1997, **70**, 3146.
- 25 T. J. Davies, R. R. Moore, C. E. Banks and R. G. Compton, *J. Electroanal. Chem.*, 2004, **574**, 123.

- 26 P. Leduc and D. Thevenot, *J. Electroanal. Chem.*, 1973, **47**, 543.
- 27 Z. Wu, W. Jing and E. Wang, *Electrochem. Commun.*, 1999, **1**, 545.
- 28 H. R. Zare and S. M. Golabi, *J. Solid State Electrochem.*, 2000, **4**, 87.
- 29 C. E. Banks, R. R. Moore, T. J. Davies and R. G. Compton, *Chem. Commun.*, 2004, 1804.
- 30 A. J. Bard and L. Faulkner, *Electrochemical Methods: Fundamentals and Applications*, John Wiley and Sons, New York, 2001.
- 31 R. R. Moore, C. E. Banks and R. G. Compton, *Anal. Chem.*, 2004, **76**, 2677.
- 32 C. E. Banks, T. J. Davies, G. G. Wildgoose and R. G. Compton, *Chem. Commun.*, 2005, 829 and references therein.
- 33 N. S. Lawrence, R. P. Deo and J. Wang, *Electroanalysis*, 2005, **17**, 65.
- 34 C.-X. Cai, H.-X. Ju and H.-Y. Chen, *Anal. Chim. Acta*, 1995, **310**, 145.
- 35 D.-M. Zhou, H.-Q. Fang, H.-Y. Chen, H.-X. Ju and Y. Wang, *Anal. Chim. Acta*, 1996, **329**, 41.
- 36 A. Santos, L. Gorton and L. T. Kubota, *Electrochim. Acta*, 2002, **47**, 3351.
- 37 S. M. Golabi, H. R. Zare and M. Hamzehloo, *Electroanalysis*, 2002, **14**, 611.
- 38 F. Pariente, F. Tobalina, M. Darder, E. Lorenzo and H. D. Abruna, *Anal. Chem.*, 1996, **68**, 3135.
- 39 Q. Gao, X. Cui, F. Yang, Y. Ma and X. Yang, *Biosens. Bioelectron.*, 2003, **19**, 277.